

Stoichiometric hydroxyapatite obtained by precipitation and sol gel processes

C. Guzmán Vázquez, C. Piña Barba, and N. Munguía
Instituto de Investigaciones en Materiales, UNAM,
Ciudad Universitaria, Apartado Postal 70-360 México 04510 D.F.,
e-mail: caroguz@servidor.unam.mx,
mcpb@servidor.unam.mx,
muna@servidor.unam.mx

Recibido el 22 de noviembre de 2004; aceptado el 3 de marzo de 2005

Three methods for obtaining hydroxyapatite (HA) are described. HA is a very interesting ceramic because of its many medical applications. The first two precipitation methods start from calcium and phosphorous compounds, whereas the third method is a sol-gel process that uses alcoxides. The products were characterized and compared. The observed differences are important for practical applications.

Keywords: Hydroxyapatite; sol-gel; calcium phosphate; ICP-UES.

Se describen tres métodos para obtener hidroxiapatita (HA). La HA es una cerámica muy interesante por sus múltiples aplicaciones médicas. Los primeros dos métodos de precipitación parten de compuestos de calcio y fósforo, mientras que el tercer método es un proceso sol-gel que usa alcóxidos. Los productos fueron caracterizados y comparados entre sí. Las diferencias observadas son importantes para aplicaciones prácticas.

Descriptores: Hidroxiapatita; sol-gel; fosfato de calcio; ICP-UES.

PACS: 81.20 Fw; 81.40-z

1. Introduction

In the last 30 years, the synthesized calcium phosphate compounds have generated a great deal of interest because of the wide variety of their medical applications, specially in orthopedics and plastic and dental surgery. These bioceramics are biocompatible and bioactive because they display links with bone. Among these compounds hydroxyapatite, HA [$\text{Ca}_{10}(\text{PO}_4)_6(\text{OH})_2$] has the chemical structure of the mineral component of bones.

HA is widely used to repair, fill, extend and reconstruct damaged bone tissue. It can also be used in soft tissue. This material can be obtained from mammal bones or coral. In the lab, it can be synthesized by reactions in solid state (1), coprecipitation (2,3), hydrothermal methods (4), or sol-gel process (5-11), among others. Precipitation in aqueous solutions is the experimental procedure most employed because HA is insoluble in water.

The molar ratio of calcium to phosphorus Ca/P varies from 1.2 to almost 2 in HA. The stoichiometric molar ratio of HA is 1.67; however, this is not the value observed in the organism because small amounts of other materials such as carbon, nitrogen, iron and another elements are incorporated. Thus, the general chemical formula is $\text{Ca}_{10-x}(\text{HPO}_4)_x(\text{PO}_4)_{6-x}(\text{OH})_{2-x}$ where $0 \leq x \leq 2$ (12,13).

Kay, Young and Posner (14) determined the crystal structure of HA. At the beginning of the 70's, it was shown that HA displayed two crystalline systems (15,16), hexagonal and monoclinic. HA contained in teeth and bones and mineral HA present a hexagonal structure; instead of dental enamel HA has a monoclinical structure. HA obtained in the lab presents a structure which depends on the of method synthesis.

The aim of this work was to synthesize HA by precipitation and sol-gel processes, and to characterize and compare the products.

2. Materials and Methods

Synthesis

2.1. First precipitation process

In order to obtain HA by precipitation, the method proposed by Rathje, Hayek, and Newesely(17) was followed. They employed calcium and phosphorus precursors in solutions. The experimental development involved the addition of 100 mL of a solution of 0.6 M of phosphoric acid (H_3PO_4) (Merck, 85%) to 100 mL of a suspension of 1.0 M calcium hydroxide ($\text{Ca}(\text{OH})_2$) (J.T.Baker, 97%) at a speed of 7 mL/min. The chemical equation that describes the reaction is:

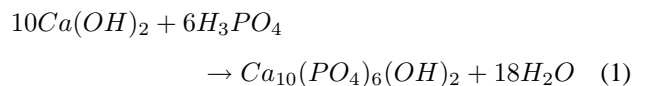


Figure 1 shows the first experimental precipitation process. A digital potentiometer Orion Mod. 1520 was used to measure the pH of the solution during mixing and aging. The mixture was warmed to 90°C for 1 hour to activate the chemical reaction and then stirred for another hour. During aging at room temperature, the HA was precipitated, filtered and washed with distilled water. The dried powder was calcined at up to 850°C for 4 to 6 hours; the obtained product was crystalline.

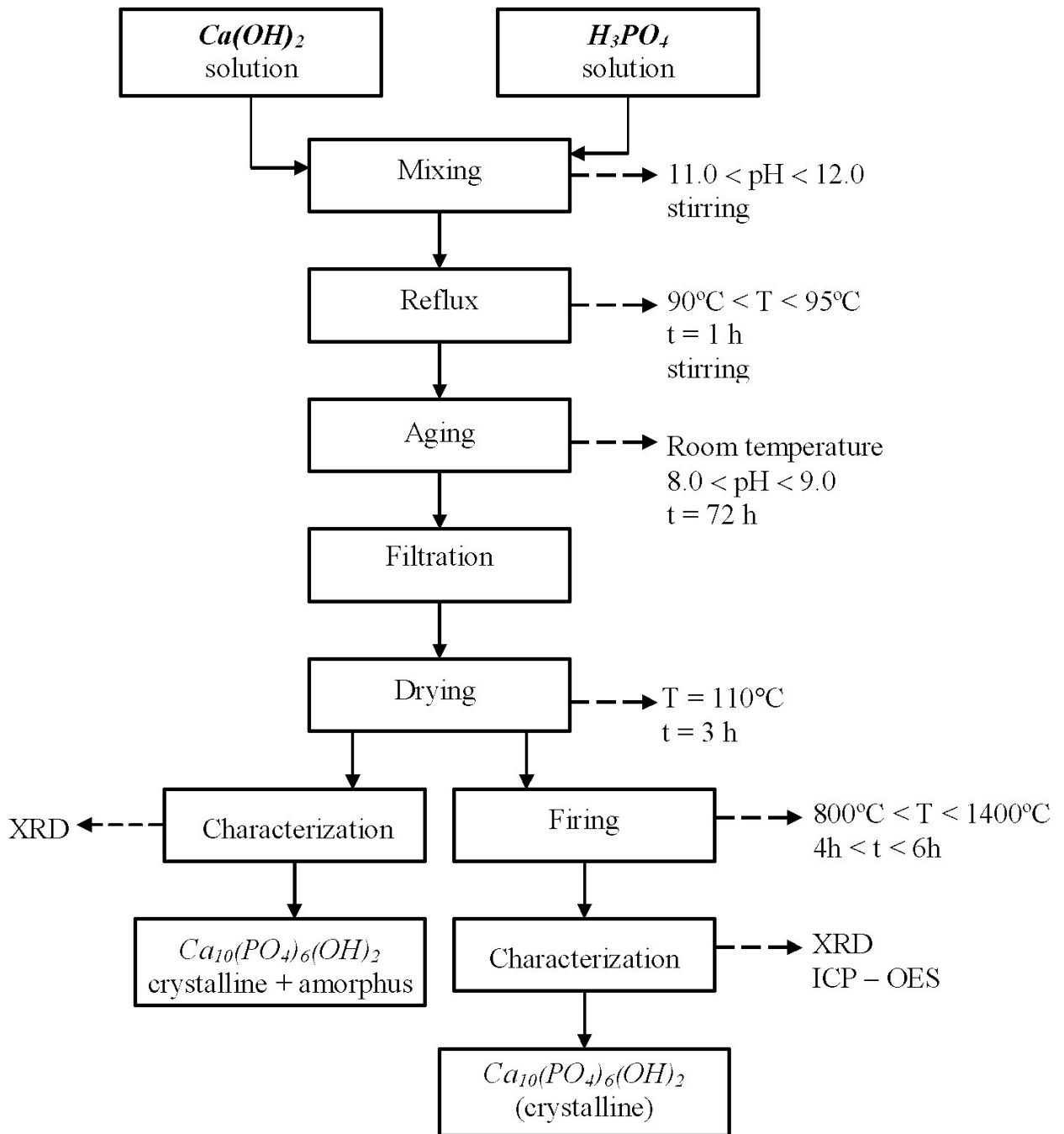
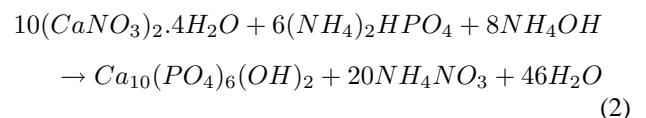


FIGURE 1. Flow chart for the synthesis of HA by precipitation process.

2.2. Second precipitation process

The method described by Hayeck and Stadlman was followed (17). The starting reagents were tetrahydrated calcium nitrate (J.T.Baker, 99,9%), phosphate monoacid of diamonio (J.T. Baker, 98,5%) and ammonium hydroxide (J.T.Baker 20-30%). In an Erlenmeyer flask containing 300 mL of 1 M of $\text{Ca}(\text{NO}_3)_2 \cdot 4\text{H}_2\text{O}$ solution, 200 mL of 0.6 M of $(\text{NH}_4)_2\text{HPO}_4$ solution was added at a rate of 22 mL/min, and 14 mL of NH_4OH , maintaining the system at 95°C with constant stirring for one hour, (Fig. 2).

The equation of the chemical reaction is:



The mixture was aged for 14 days at room temperature. After this period, the obtained precipitate was filtered and washed several times with distilled water. Then it was dried at 250°C for 3 hours and calcined at 850°C.

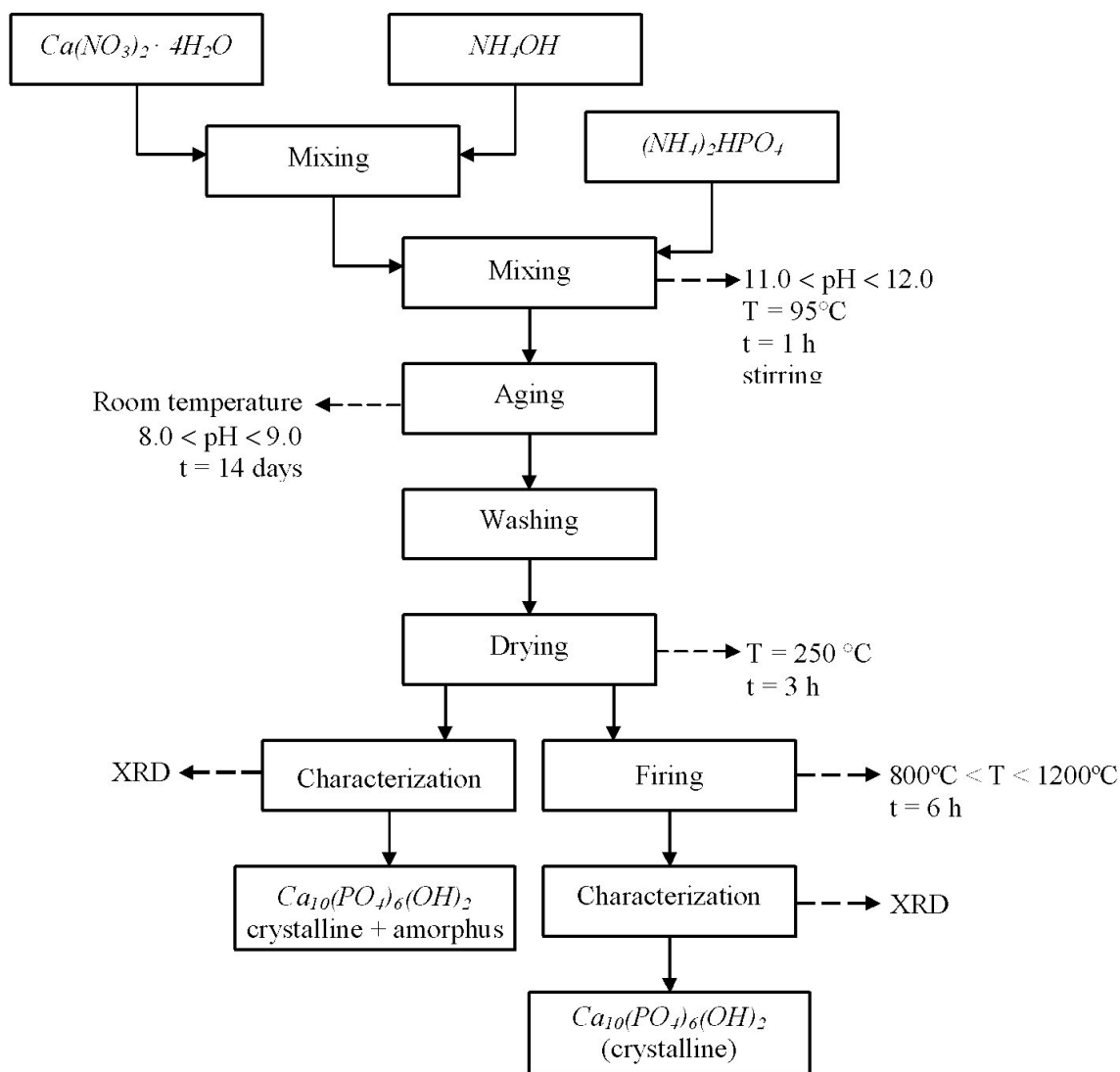
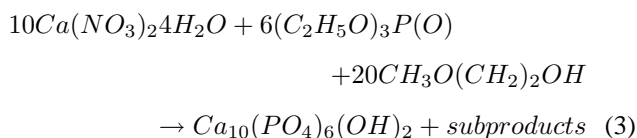


FIGURE 2. Flow chart for the synthesis of HA by a second precipitation process.

2.3. Sol-gel (PSG) Process

Triethyl phosphate (Aldrich, 99.8%) and calcium nitrate tetrahydrated (Baker, 99.9%) were used, as well as 2-metoxiethanol ether (Aldrich, 99.3%) as an organic solvent. Esther phosphate was hydrolyzed with the release of water during the first stage of the reaction, generating HA (18).

The equation of the chemical reaction is:



In order to obtain a Ca/P ratio of 1.667, 23.483g of $Ca(NO_3)_2 \cdot 4H_2O$, 10.2 mL of $(C_2H_5O)_3P(O)$ and 15.6 mL of $CH_3O(CH_2)_2OH$ were used. The container was closed and constantly stirred until a homogenous mixture was obtained.

Figure 3 shows the procedure. Calcium nitrate tetrahydrated crystals and 2-metoxiethanol were placed in a closed Erlenmeyer flask, stirring, and then triethyl phosphate was added. The mixture was aged for 4 days at 80°C with stirring. To start the gelation process the flask was opened and the temperature increased to 90°C < T < 100°C. At the end of this stage there was a very viscous yellowish gel, which that was dried to obtain a grayish product and then washed. Finally it was calcined for 12h at 1200°C and HA was obtained.

Characterization

2.4. X-ray diffraction analysis

The products were characterized by X-ray diffraction with a Bruker AXS Diffract Plus/D8 Advance, using $CuK\alpha$ radiation (1.5418 Å), 35 kV and 30 mA. HA, $CaCO_3$, $Ca(NO_3)_2$

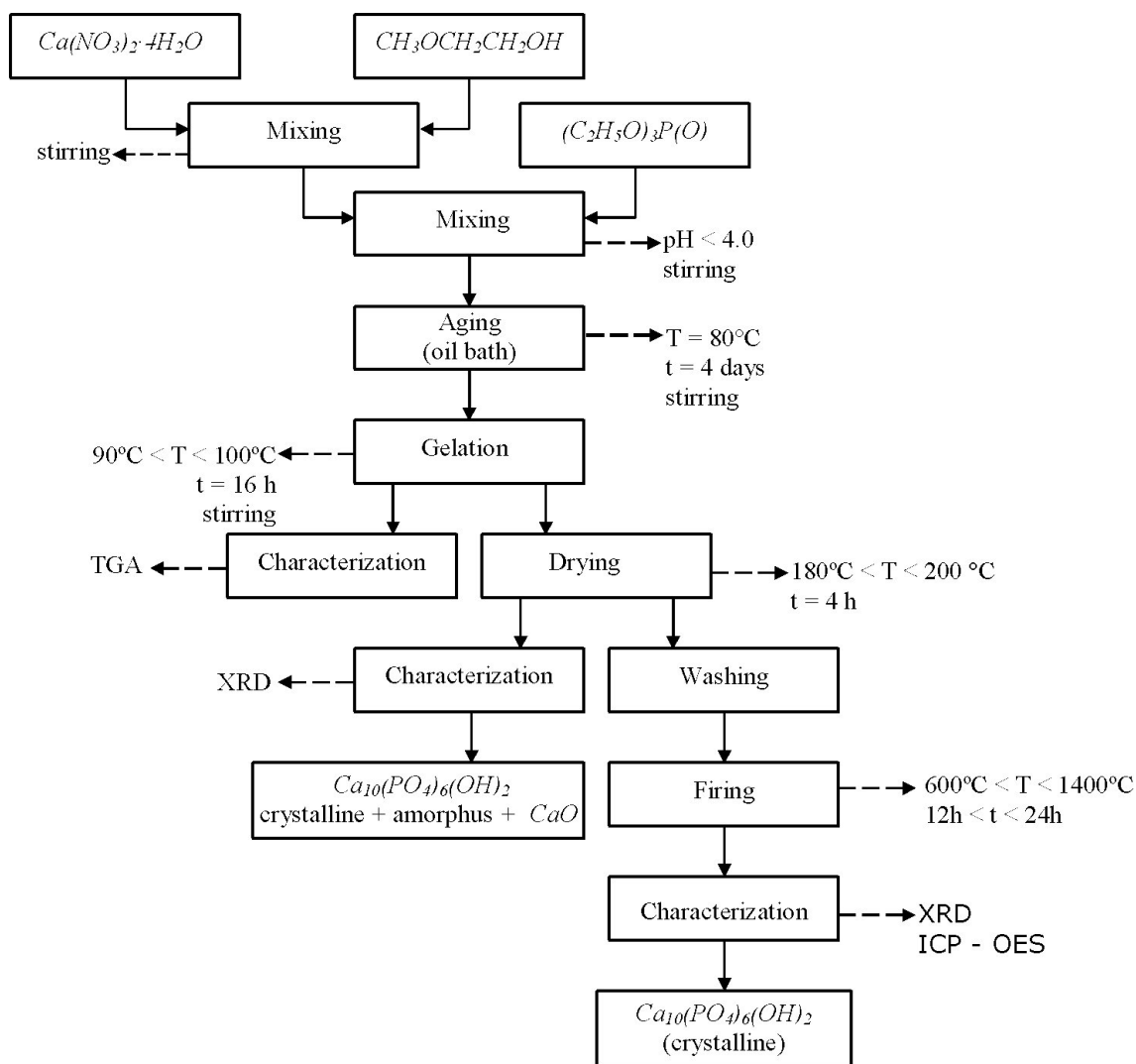


FIGURE 3. Flow chart for obtaining HA by the sol gel process.

and β -TCP or whitlockite were identified by comparing with the JCPDS files.

2.5. Thermogravimetric Analysis (TGA)

The gel produced by the sol-gel process was studied by TGA to determine the mass variation in the sample. The sublimation temperatures of volatile substances were determined by DTA. A Hi-Tes TGA 2959 Thermogravimetric Analyzer was used, the temperature interval was $1000^{\circ}\text{C} \geq T \geq T_{\text{room}}$, the heating rate was $5^{\circ}\text{C}/\text{min}$ under nitrogen flow.

2.6. Measure of Ca/P by ICP-OES

The Ca/P molar ratio was determined by inductively connected plasma with optical emission spectroscopy (ICP-OES). A Perkin Elmer Optimal 4300DV instrument was used. 0.1g of the sample was digested in an acid sample made up of 2.5 mL of HNO_3 , 1.5 mL of H_2O_2 and 0.3 mL of HCl in a 100 mL Erlenmeyer flask. The Ca and of the P wave-

lengths were used. The measurements of the concentration were made by triplicate on three different days. The concentration of Pb, Cd, As and Hg was also determined.

Scanning Electronic microscopy (SEM)

The microstructure of the crystals was determined using a Lica Cambridge Stereoscan 440, and the samples were covered with gold. The size of clusters of particles was determined as well.

3. Results

3.1. X-ray diffraction analysis

Figures 4 and 5 show the X-ray diffraction patterns of the dried product before and after calcinations, for two precipitation processes. In both cases there is only HA.

Figure 6 shows X-ray diffraction pattern of the sol-gel product after drying for 4 hrs at $180^{\circ}\text{C} \geq T \geq 200^{\circ}\text{C}$ (a) and after calcination at 600°C (b) and 800°C (c). In this case, CaO and CaCO_3 were also formed.

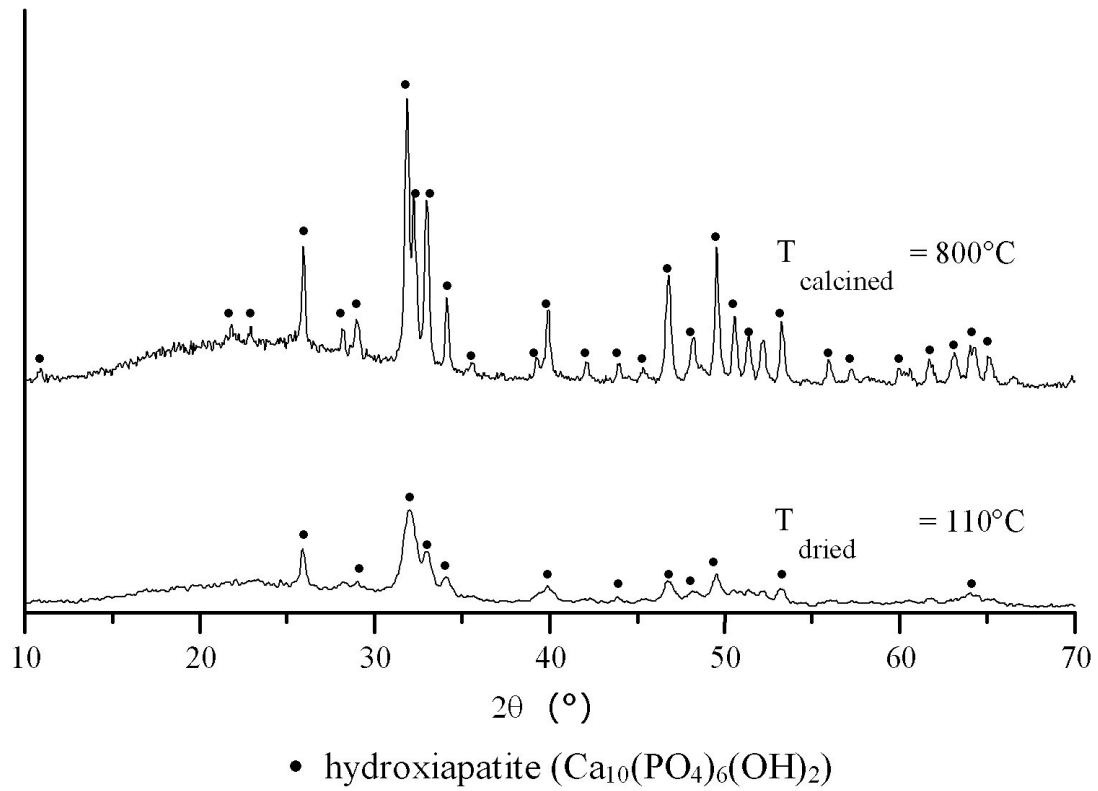


FIGURE 4. XRD of the sample obtained by the first precipitation process.

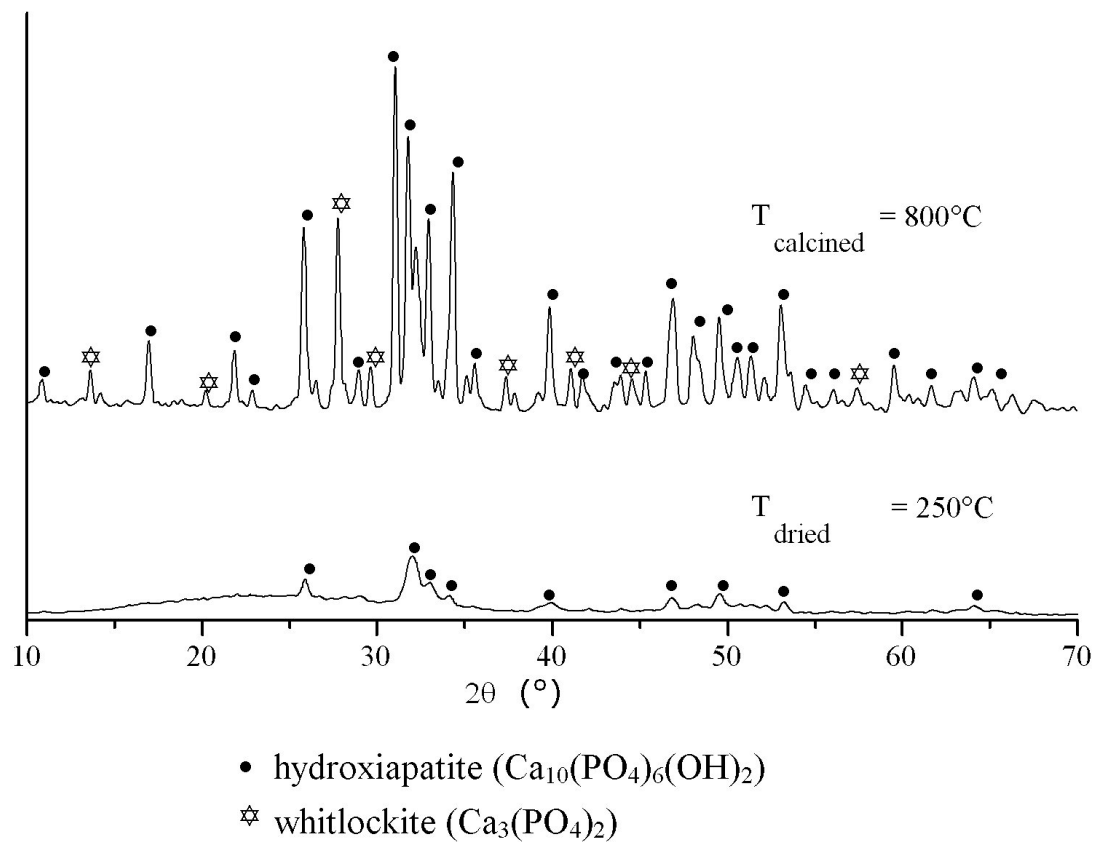


FIGURE 5. XRD of the sample synthesized by the second precipitation process.

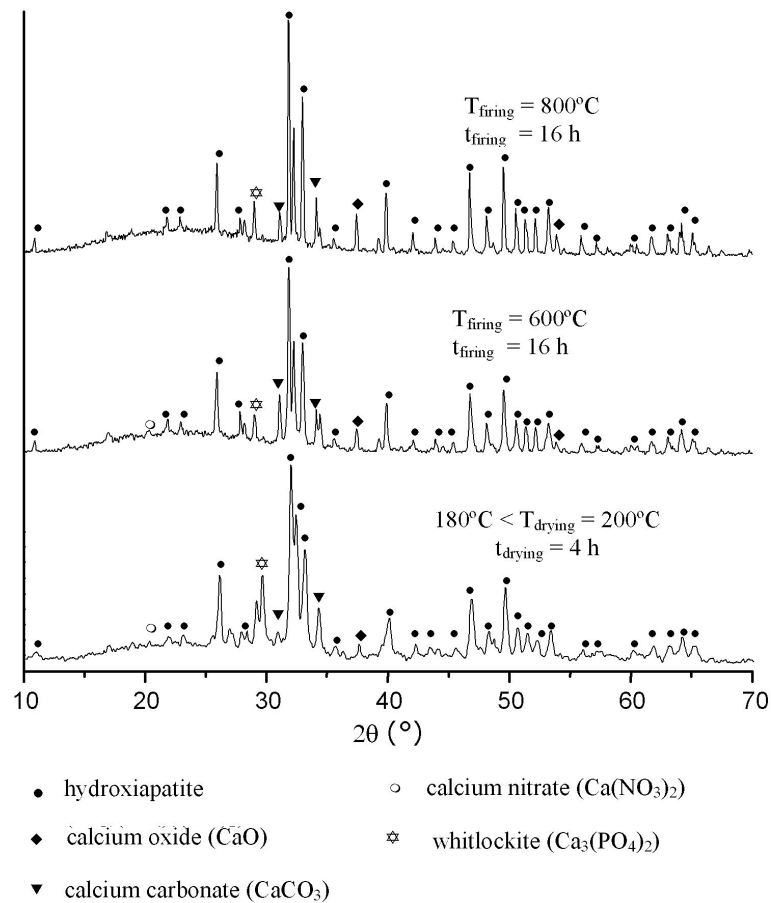


FIGURE 6. XRD of sample obtained by the Sol-gel process, after drying 4h, $180 < T < 200^{\circ}\text{C}$ (a); after calcinations during 16h at 600°C (b); and at 800°C (c).

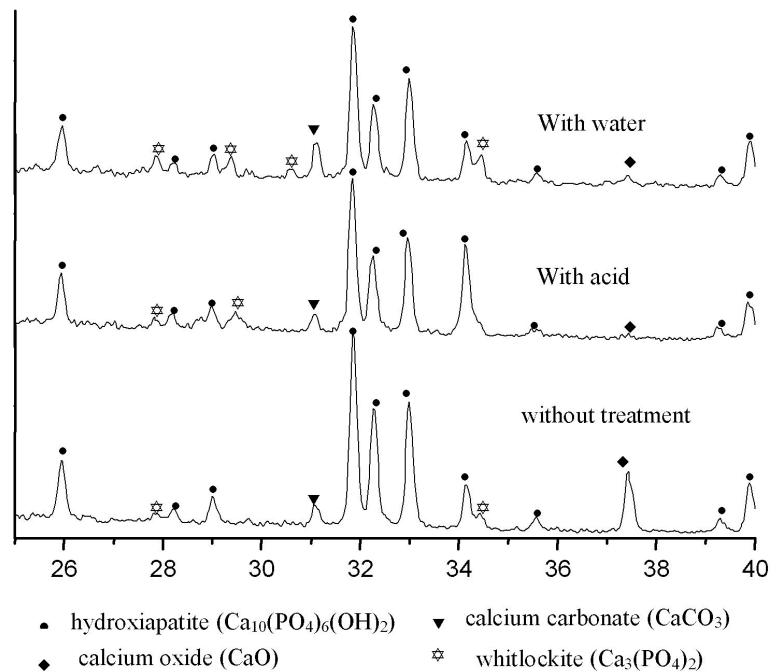


FIGURE 7. XRD of the sample without chemical treatment (a); with chemical treatment to eliminate CaO . CaO (◆) and CaCO_3 (▼) appears.

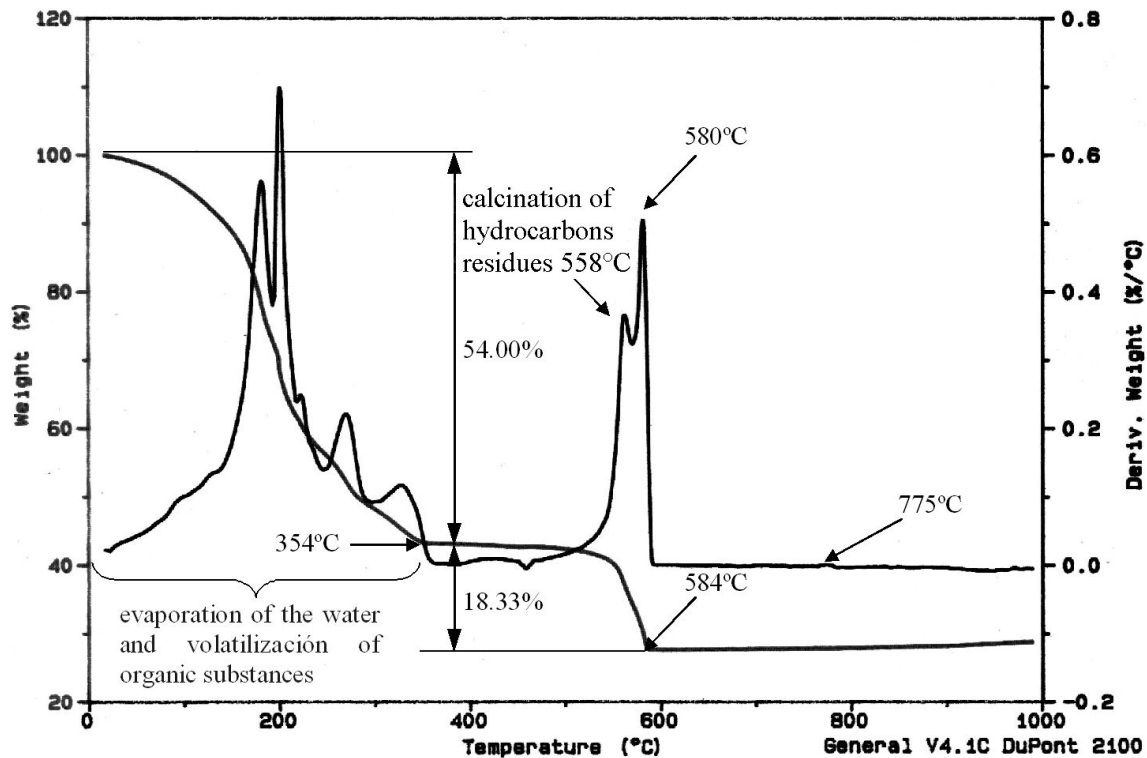


FIGURE 8. TGA and DTA of the sample obtained by sol-gel process.

TABLE I. Ca and P concentrations in the different processes reported.

Technique	Ca ($\mu\text{g mL}^{-1}$)	P ($\mu\text{g mL}^{-1}$)	Ca/P Ca/P	Average
First process by precipitation	357.98	175.58	2.04	2.04
	368.90	181.72	2.03	
	383.50	186.70	2.05	
Second procedure by precipitation	373.02	175.72	2.12	2.10
	372.53	178.54	2.08	
	378.13	180.60	2.09	
sol-gel process	412.04	191.27	2.15	2.17
	406.54	186.38	2.18	
	416.60	189.85	2.19	
Natural bovine bone	347.90	177.31	1.96	1.97
	398.21	204.74	1.94	
	389.66	197.69	1.97	

The sample was washed to several times with distilled water remove CaO phase. Figure 7 shows the X-ray diffractograms of HA after the chemical treatments to remove CaO phase.

3.2. Thermogravimetric Analysis (TGA)

Figure 8 corresponds to the thermogravimetric analysis (TGA) and differential thermal analysis (DTA) of the gel

obtained by the sol-gel procedure. There are two stages of mass loss. The first one is of 54% at $364^{\circ}\text{C} \geq T \geq T_{\text{room}}$ and the second, of 18.33% at $584^{\circ}\text{C} \geq T \geq 500^{\circ}\text{C}$. There is an initial loss due to water evaporation and methanol (CH_3OH) combustion, both at less than 100°C . Calcination of the $\text{Ca}(\text{OCH}_3)_2$ occurs at *ca.* 180°C . The decomposition of nitrogenated substances as NO_x and the formation of calcium carbonate occur. Over the temperature interval $350^{\circ}\text{C} < T < 550^{\circ}\text{C}$ there is a very slight slope attributed to the release of gas inside the sample. Exothermic processes, registered at $550^{\circ}\text{C} < T < 590^{\circ}\text{C}$, show the crystallization of HA. The small peak located at 775°C corresponds to the decomposition of CaCO_3 .

TABLE II. Trace element concentrations in the different samples obtained.

Sample	Pb ($\mu\text{g mL}^{-1}$)	Cd ($\mu\text{g mL}^{-1}$)	As ($\mu\text{g mL}^{-1}$)	Hg ($\mu\text{g mL}^{-1}$)
First procedure by precipitation	6.5	1.6	0.71	0.28
Second procedure by precipitation	5.5	1.6	0.24	0.32
Sol - gel process	3.3	1.4	0.61	0.07
Natural bovine bone	162.5	1.6	0.42	0.48

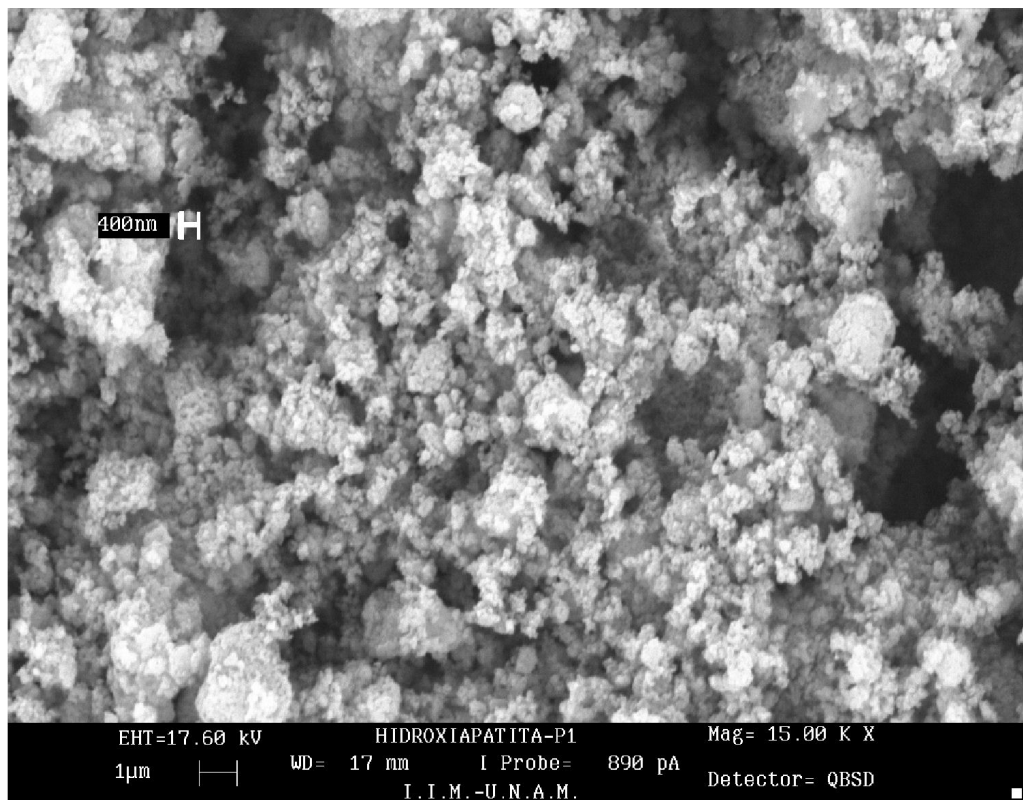


FIGURE 9. Microstructure of the sample obtained by the first precipitation process.

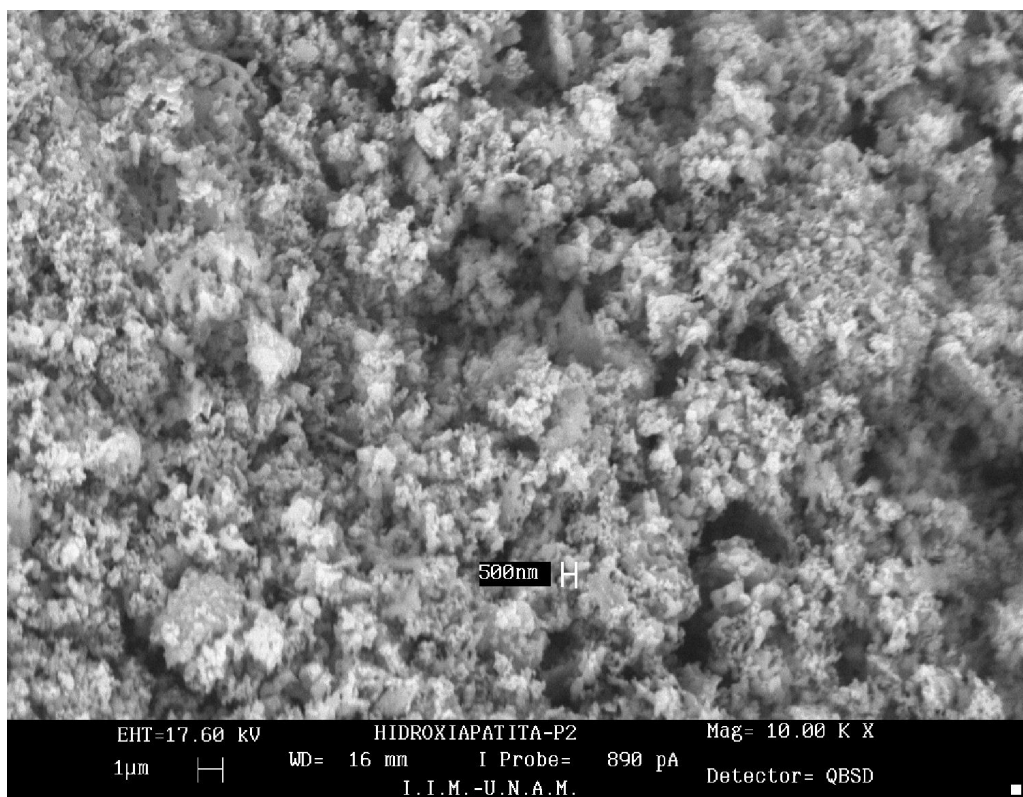


FIGURE 10. Microstructure of the sample obtained by the second precipitation process.

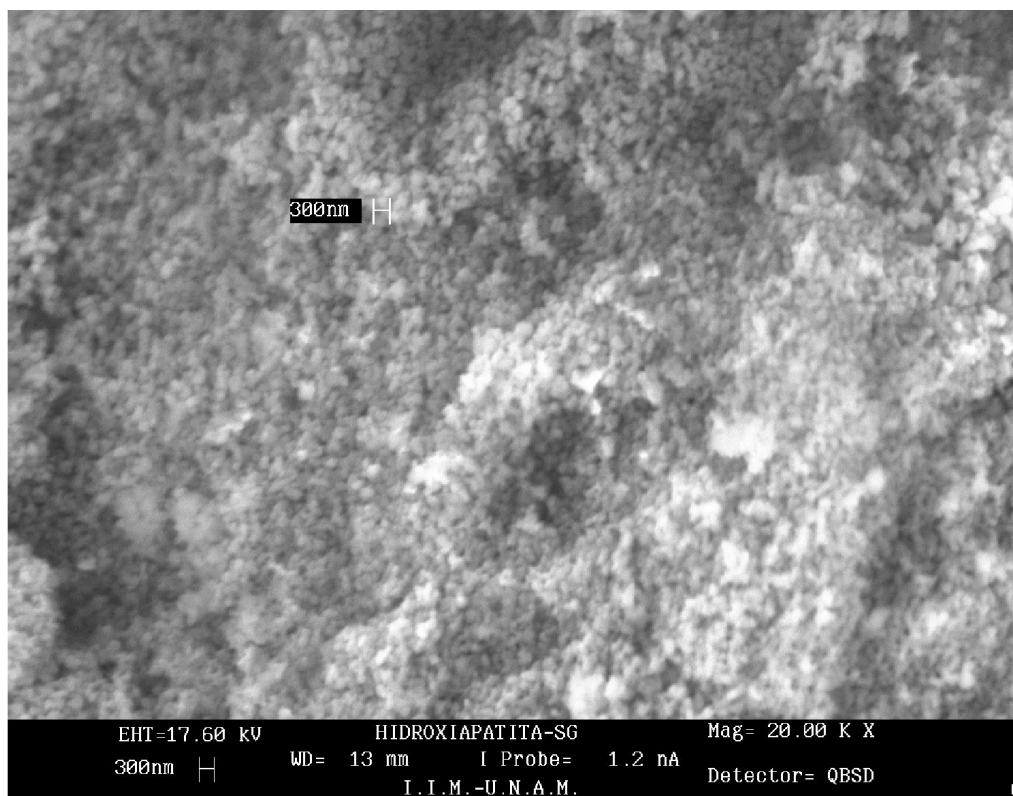


FIGURE 11. Microstructure of the sample obtained by the sol-gel process.

TABLE III. Trace elements allowed by the ASTM 1185-1188 standard.

Elements	Pb	Cd	As	Hg
Maximum limit (ppm)	30	5	3	5
Q. L. ($\mu\text{g mL}^{-1}$)*	0.020	0.012	0.010	0.025
D.L. ($\mu\text{g mL}^{-1}$)**	0.006	0.004	0.002	0.008

* Q. L, quantifiable limit of the element, is equivalent to 10 times the noise of the equipment.

** D. L, detectable limit of the element, is equivalent to 3 times the noise of the equipment.

3.3. Ca/P molar ratio determination by ICP-OES

Results of Ca and P concentrations for HA obtained by three processes are shown in Table I. The results corresponding to Pb, Cd, As and Hg are shown in Table II. In Table III the maximum values allowed for these elements according to the norm ASTM F1185-1188, for medical applications of HA, are shown.

3.4. Scanning electron microscopy (SEM)

The micrographs of the samples obtained through different procedures are shown in Figs. 9 to 11. Clusters of HA particles have a homogenous size. The average size of the clusters was 400 nm for the first precipitation procedure $[\text{Ca}(\text{OH})_2 + \text{H}_3\text{PO}_4]$, 500 nm for the second

$[\text{Ca}(\text{NO}_3)_2 \cdot 4\text{H}_2\text{O} + \text{NH}_4\text{OH} + (\text{NH}_4)_2\text{HPO}_4]$ and 300nm for the sol-gel process.

4. Discussion and conclusions

Although the precipitation processes to obtain HA depend on variables such as pH, time of aging, temperature, etc., they are more effective and less expensive than the sol-gel process; crystalline HA is obtained and the yield is better compared to the sol-gel process. The first precipitation process produces a more crystalline HA than the second process.

HAs obtained by precipitation processes are nonstoichiometric, with a Ca/P ratio < 1.67 , whereas the one obtained by the sol-gel process is stoichiometric. Concentrations of Pb, Cd, As and Hg are lower than those stipulated for medical applications. The HA obtained by the sol-gel process has a very high level for purity, a homogenous composition and smaller cluster size.

We conclude that each of the processes for obtaining HA has its favorable qualities, and therefore it is important to choose the best one depending on the application.

Acknowledgements

To M. in Sc. Jaime Santoyo, Q. Leticia Baños, Q. Carmen Vázquez, Tech. Carlos Flores, Mr. Eduardo Caballero for their technical support. To Ph. D. Pedro Bosch and M. Sc. Angeles Aguilar for their advice.

1. Rao R. Ramachandra, H.N. Roopa, and T.S. Kannan, *J. Mater. Sci. Mater. Med.* **8**(1997) 511.
2. Tas A. Cuney, F. Korkusuz, M. Timicin, and N. Akkas, *J. Mater. Sci. Mater. Med.* **8** (1997) 91.
3. S.H. Rhee and J. Tanaka, *J. Am. Ceram. Soc.* (1998) 3029.
4. H.S. Liu *et al.*, *Ceram. Int.* **23** (1997) 19.
5. P. Layrolle, A. Ito, and T. Tateishi, *J. Am. Ceram. Soc.* **81** (1998) 1421.
6. G. Kordas and CC. Trapalis, *J. Sol-gel Sci. Tech.* **9** (1997) 17.
7. A. Jilavenkatesa and Sr RA. Condrate, *J. Mater. Sci.* **33** (1998) 4111.
8. A. Jilavenkatesa, D.T. Hoelzer, and RA. Condrate, *J. Mater. Sci.* **34** (1999) 4821.
9. M.F. Hsieh, L.H. Perng., T.S. Chin, and H.G. Perng, *Biomaterials* **22** (2001) 2601.
10. M.F. Hsieh, L.H. Perng, and T.S. Chin, *J. Sol-gel Sci. Tech.* **23** (2002) 205.
11. K.A. Gross, C.S. Cah, G.S.K. Kannangara, and B. Ben Nissan. *J. Mater. Sci. Mater. Med.* **9** (1998) 839.
12. A. Slosarczyk, E. Stobierska, Z. Paskiewicz and M. Gawlicki, *J. Am. Ceram. Soc.* **79** (1996) 2539.
13. T. Yamamuro, L.L. Hench, and J. Wilson, *CRC Handbook of Bioactive Ceramics*, Vol.II: Calcium phosphate and hidroxiapatite ceramic (CRC Press Inc., Boca Raton, Florida, 2000).
14. M.I. Kay, R.A. Young, and A.S. Posner, *Nature* **204** (1964) 1050.
15. J.C. Elliot, P.E. Mackie, and R.A. Young, *Science* **180** (1973) 1055.
16. T.S.B. Narasaraju and D.E. Phebe, *J. Mat. Sc.* **31** (1996) 1.
17. L. Hench and J. Wilson, *An Introduction to Bioceramics* (World Scientific London, U.K., 1993).
18. A. Jilavenkatesa and R.A. Condrate, *J. Mater. Sc.* **33** (1998) 4111.